PALEOCEANOGRAPHY, VOL. 14, NO. 1, PAGES 84-95, FEBRUARY 1999

Terrigenous flux in the Rio Grande Rise area during the past 1500 ka: Evidence of deepwater advection or rapid response to continental rainfall patterns?

Franz X. Gingele,[1] Frank Schmieder,[2] Tilo von Dobeneck,[2] Rainer Petschick,[3] and Carsten Rühlemann[2]

Abstract. Surface sediment samples and three gravity cores from the eastern terrace of the Vema Channel, the western flank of the Rio Grande Rise, and the Brazilian continental slope were investigated for physical properties, grain size, and clay mineral composition. Discharge of the Rio Doce is responsible for kaolinite enrichments on the slope south of 20° and at intermediate depths of the Rio Grande Rise. The long-distance advection of kaolinite with North Atlantic Deep Water from lower latitudes is of minor importance as evidenced by low kaolinite/chlorite ratios on the Mid-Atlantic Ridge. Cyclic variations of kaolinite/chlorite ratios in all our cores, with maxima in interglacials, are attributed to low- and high-latitude forcing of paleoclimate on the Brazilian mainland and the related discharge of the Rio Doce. A long-term trend toward more arid and "glacial" conditions from 1500 ka to present is superimposed on the glacial-interglacial cyclicity.

1. Introduction

The Rio Grande Rise/Vema Channel/Hunter Channel region is a key area in the western South Atlantic to study spatial as well as temporal variations in the history of deepwater masses. Southern source bottom water passes from the Argentine to the Brazil Basin via the Vema and Hunter Channels. Above, southward flowing North Atlantic Deep Water (NADW) is recorded from 4000 to 2000 m water depth, overlain by Upper Circumpolar Water (UCPW) and Antarctic Intermediate Water (AAIW) [*Peterson and Stramma*, 1990]. The Rio Grande Rise (RGR), which reaches water depths of 800 m, offers the opportunity to sample sediments situated in different water masses and look for tracers of changes in thermohaline circulation.

Numerous studies have focussed in particular on variations in the propagation of Antarctic Bottom Water (AABW) and NADW in the South Atlantic using various tracers from benthic foraminifera assemblages [*Mackensen et al.*, 1993; *Schmiedl and Mackensen*, 1997], Cd/Ca ratios in benthic foraminifera [*Boyle*, 1988, 1994; *Oppo and Rosenthal*, 1994], carbon-13 composition [*Curry et al.*, 1988; *Duplessy et al.*, 1988; *Mackensen et al.*, 1994], diatoms [*Jones and Johnson*, 1984], grain size [*Massé et al.*, 1994], and clay minerals [*Biscaye*, 1965, *Chamley*, 1975, *Jones*, 1984; *Diekmann et al.*, 1996].

On the basis of their strong latitudinal and reciprocal distribution patterns in surface sediments of the South Atlantic, kaolinite and chlorite were inferred to be useful tracers of the major deepwater masses in the vicinity of the RGR. An advection of chlorite with southern source deepwater (AABW) was found by *Biscaye* [1965] and confirmed by later studies [*Jones*, 1984; *Petschick et al.*, 1996]. The occurrence of a kaolinite maximum at intermediate depths (above 4000 m) was attributed to advection of this mineral by NADW [*Chamley*, 1975]. The propagation of kaolinite with NADW is a well-documented feature in many cores from the eastern South Atlantic [*Diekmann et al.*, 1996].

Alternatively, *Jones* [1984] suggested an isopycnal transport model for the kaolinite enrichment on the RGR. On the basis of the assumption that the suspension load of the NADW in the western South Atlantic is too small to sustain a substantial enrichment (clearwater minimum), kaolinite input by the Rio Doce, southward transport with the Brazil current, deposition on the Sao Paulo (Santos) Plateau, and resuspension and isopycnal flow to the RGR was proposed. These different interpretations have implications on the evaluation of temporal changes of kaolinite content in sediment cores, which record either oceanic processes such as NADW fluctuations, sea level changes, or variations in fluvial discharge.

We examined 51 surface samples from two transects to evaluate potential sources and recent propagation of clay minerals (Figure 1). One profile samples the continental slope off the Rio Doce. The second transect runs from the slope across the Santos Plateau, the western and eastern flank of the RGR, to the Mid-Atlantic Ridge (MAR).

The temporal variation in the supply of clay minerals during the past 200 kyr was investigated in sediment cores from the slope (GeoB 2110) and the eastern terrace of the Vema Channel (GeoB 2822). A complete record of clay mineral supply covering the past 1500 kyr was found in core GeoB 2821. This core is situated in a key position on the western flank of the RGR just above the present AABW/NADW boundary. Cross-spectral analysis on the kaolinite/chlorite ratio of this core was carried out to determine phase relationships to orbital cycles and compare phase angles of related paleoceanographic and paleoclimatic proxies.

[1] Baltic Sea Research Institute, Rostock-Warnemuende, Germany.

[2] University of Bremen, Bremen, Germany.

[3] University of Frankfurt, Frankfurt, Germany.

Paper number 1998PA900012.
0883-8305/99/1998PA900012$12.00

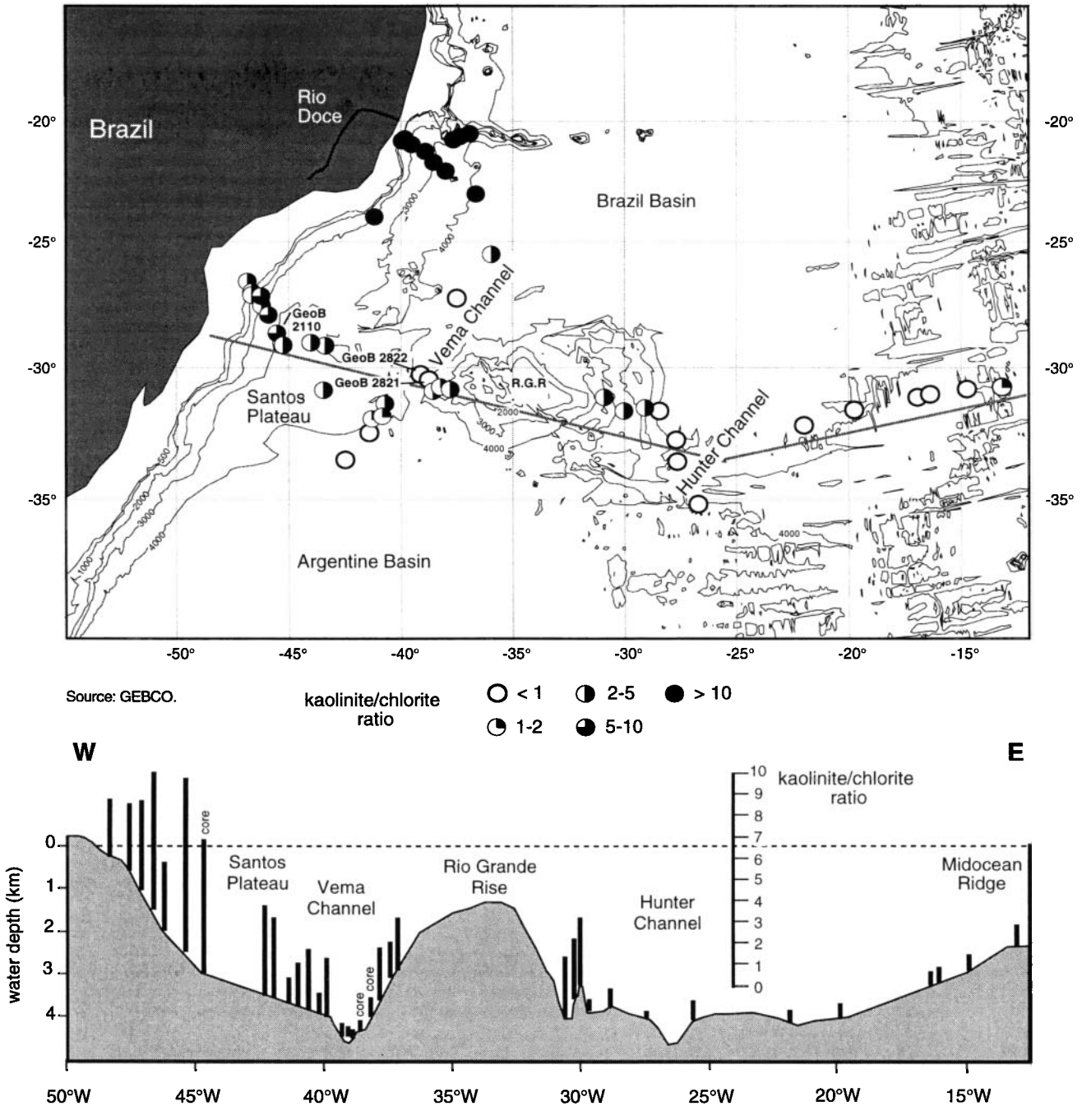

Figure 1. Area of investigation, core locations, and kaolinite/chlorite ratios of 51 surface samples in the investigation area. Depth contours after General Bathymetric Chart of the Oceans (GEBCO). Kaolinite/chlorite ratios are also projected on a hypothetical transect from the Santos Plateau across the Rio Grande Rise (RGR) to the Hunter Channel and Mid-Atlantic Ridge (MAR). Extreme kaolinite/chlorite values (>10) from sites directly off the Rio Doce are excluded from the projection.

2. Material and Methods

Sediment surface samples were recovered with giant box corer and multicorer during *Meteor* cruises M15/2 [*Pätzold et al.*, 1993], M23/2 [*Bleil et al.*, 1993], M29/2 [*Bleil et al.*, 1994], and M34/3 [*Wefer et al.*, 1996]. Sample treatment and clay mineral analyses are given in detail by *Petschick et al.* [1996]. Sediment cores (Table 1) were retrieved with a gravity corer on cruises M23/2 (GeoB 2110-3/4) and M29/2 (GeoB 2821-1 and GeoB 2822-2). Core GeoB 2110 from 3008 m water depth on the continental slope above the Santos Plateau (Figure 1) consists of grey hemipelagic clays with varying amounts of carbonate. Core GeoB 2822 from the eastern terrace of the Vema Channel (4267 m water depth) comprises terrigenous muds with small amounts of calcareous nannofossils and foraminifera. Increasing amounts of carbonate characterize core GeoB 2821 from the western flank of the RGR (3927 m water depth).

Table 1. Location of Sediment Cores

Core	Water Depth, m	Latitude, Longitude	Cruise Report	Age Model
GeoB 2110-3/4	3008	28°38.9'S, 45°31.2'W	*Bleil et al.* [1993]	*Bleil et al.* [1993] and C. Rühlemann, (unpublished data, 1993)
GeoB 2821-1	3927	30°27.1'S, 38°48.1'W	*Bleil et al.* [1994]	F. Schmieder, (unpublished data, 1994)
GeoB 2822-2	4267	30°14.3'S, 39°08.5'W	*Bleil et al.* [1994]	*Bleil et al.* [1994]

The cores were sampled at 5 cm intervals. Samples were treated with 10% acetic acid to remove carbonate, sieved over a 63 μm mesh, and split into >2 μm and <2 μm fractions by settling technique. The weight percentage of the sand fraction (>63 μm) was negligible. Weight percentages of the silt (2-63 μm) and clay fraction (<2 μm) were used to compute a silt/clay ratio. The clay fraction (<2 μm) was analyzed by X-ray diffraction (CoK_α radiation) on oriented mounts for the four clay mineral groups kaolinite, smectite, illite, and chlorite following standard procedures given in detail by *Petschick et al.* [1996]. These procedures assume that the four main clay mineral groups add up to 100% in the fraction <2 μm and involve the use of the weighting factors of *Biscaye* [1965]. As a consequence our absolute percentages for the individual clay minerals cannot be compared to those of *Jones* [1984], who used weighting factors of *Heath and Pisias* [1979]. However, general patterns of clay mineral distribution are similar.

Magnetic susceptibility was measured on the archive halves of the cores at a 1 cm spacing using a Bartington Instruments M.S.2.C loop sensor. Lomb-Scargle Fourier transform [*Lomb*, 1976; *Scargle*, 1982, 1989] embedded in the Spectrum program [*Schulz and Stattegger*, 1997] was used for all spectral analysis. This spectral estimation method can be directly applied to unevenly spaced geological times series. Cross-spectral analysis for GeoB 2821 was performed using *Welch's* [1967] overlapped segment average (WOSA) procedure to reduce spectral peaks originating from random fluctuations.

2.1. Stratigraphy of GeoB 2110

A preliminary stratigraphic framework was established on shipboard counts of the planktonic foraminifera *Globorotalia menardii* [*Mulitza*, 1993]. On the basis of the cyclic appearance of this species, *Ericson and Wollin* [1968] defined a biostratigraphic zonation scheme using a letter notation from Z (Holocene) to Q in order of increasing ages. Zones Z to U can be directly correlated to oxygen isotope stages with following ages at zone boundaries: Z/Y, 12 ka; Y/X, 80 ka; X/W, 130 ka; W/V, 185 ka; and V/U, 370 ka. Though minor shifts in stage boundaries occur because of the poor resolution of the *G. menardii* counts, the preliminary stratigraphic framework was confirmed for site GeoB 2110 by carbonate stratigraphy after *Damuth* [1977]. Oxygen isotope measurements on planctic and benthic foraminifera were carried out on a Finnegan mass analyzing technique (MAT) 251 mass spectrometer (Figure 2). The measurements of the planktonic foraminifera *Globigerinoides sacculifer* were partly complicated by low sedimentation rates and enhanced carbonate dissolution but enabled identification of oxygen isotope stages 6.0, 6.2, 7.0, and 7.1. Supplementary measurements of *Uvigerina* spp. near isotope stage 4 clarified the stratigraphic position of stages 4.0 and 5.0. In addition to isotope stratigraphy, some characteristic patterns of the high-resolution magnetic susceptibility record were correlated to the SPECMAP stack [*Imbrie et al.*, 1984] and supplied four more tie points (near oxygen isotope stages 2.2, 3.0, 5.5, and 6.4). Because of different phase lags of planktonic and benthic foraminifera and magnetic susceptibility, no phase information can be deduced from this combined age model.

2.2. Stratigraphy of GeoB 2821

The *G. menardii* counts for core GeoB 2821 did not produce a reasonable pattern. This is due to the wide sample spacing of the shipboard samples and the low sedimentation rates of this core. Since no $\delta^{18}O$ stratigraphy is available an age model derived by orbital tuning of the susceptibility record was used here. This cyclostratigraphy was established in the framework of a stratigraphical synthesis of 12 sediment cores from the subtropical South Atlantic Ocean (subtropical South Atlantic susceptibility (SUSAS) stack) [*von Dobeneck and Schmieder*, 1998], based on cyclic and highly coherent magnetic susceptibility logs. The correlation of susceptibility and carbonate content is inverse as in many marine environments [e.g., *Robinson*, 1990]. This indicates that the rock magnetic signal is a result of varying dilution of the (terrigenous) magnetic sediment fraction by glacial-interglacial carbonate dissolution cycles. On the basis of a detailed stepwise alternating field demagnetization of the Natural Remanent Magnetization (NRM), three paleomagnetic age marks could be identified for GeoB 2821 (Figure 2). A simple age model generated by linear interpolation of these reversal ages already shows spectral characteristics of Milankovitch cyclicity (100 and 41 kyr cycles), suggesting climatic forcing. Correlation to a precisely dated paleoclimate record was necessary to improve the age-depth relation prior to orbital tuning. The $\delta^{13}C$ record of South Pacific Ocean Drilling Program (ODP) Site 806 (T. Bickert, unpublished manuscript, 1998) exhibits a continuously high pattern similarity with the susceptibility record of GeoB 2821 and was therefore used as age reference. The predominant 40 kyr cyclicity of susceptibility was then synchronized with astronomically calculated obliquity variations [*Berger and Loutre*, 1991] as a target curve. A phase shift of -30° (-3.4 kyr) was found by cross-spectral analysis of magnetic susceptibility and $\delta^{18}O$ for one of the SUSAS records [*von Dobeneck and Schmieder*, 1998] ($\delta^{18}O$ data by *Bickert* [1992]). This value corresponds to those calculated by *Imbrie et al.* [1993] for early proxy responses in the Southern Hemisphere. As the SPECMAP stack [*Imbrie et al.*, 1984] is assumed to lag

Figure 2. (opposite) Parameters used for the stratigraphic classification of the cores. Age models for cores GeoB 2110 and GeoB 2821 are based on shipboard counts of *Globorotalia menardii*. Oxygen isotopes in core GeoB 2110 were measured on the planctic foraminifera *Globigerinoides sacculifer* and some benthic *Uvigerina peregrina*. The stratigraphic framework of GeoB 2821 is based on paleomagnetic analyses and orbital tuning of the magnetic susceptibility record. Also depicted are kaolinite-chlorite ratios and grain size (ratio of silt/clay weight percentages), which fluctuate in a glacial-interglacial pattern. Note that the records of susceptibilty and grain size are reversed for better graphic correlation.

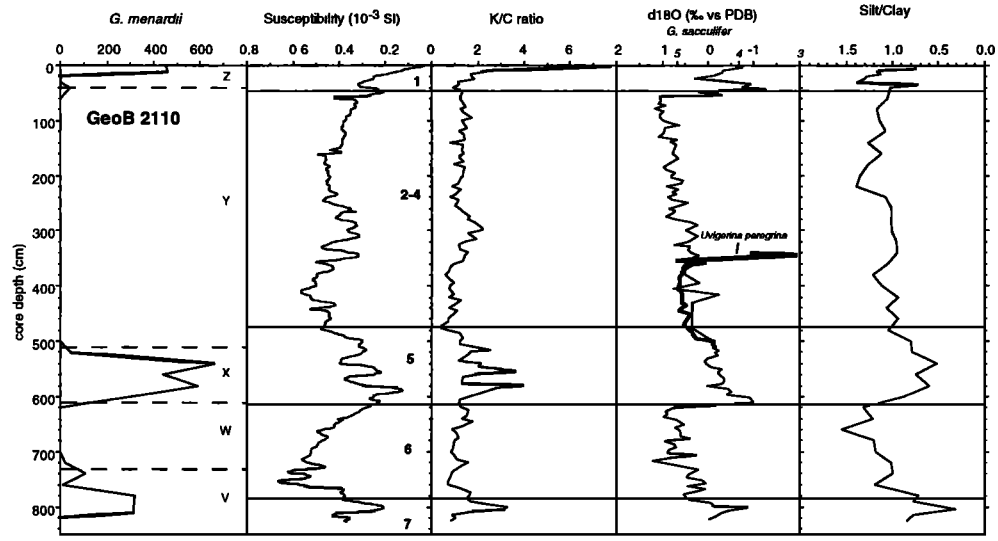
G. menardii
Susceptibility (10-3 SI)
K/C ratio
d18O (‰ vs PDB)
G. sacculifer
Silt/Clay
GeoB 2110
core depth (cm)
Z
Y
X
W
V
1
2-4
5
6
7
Uvigerina peregrina

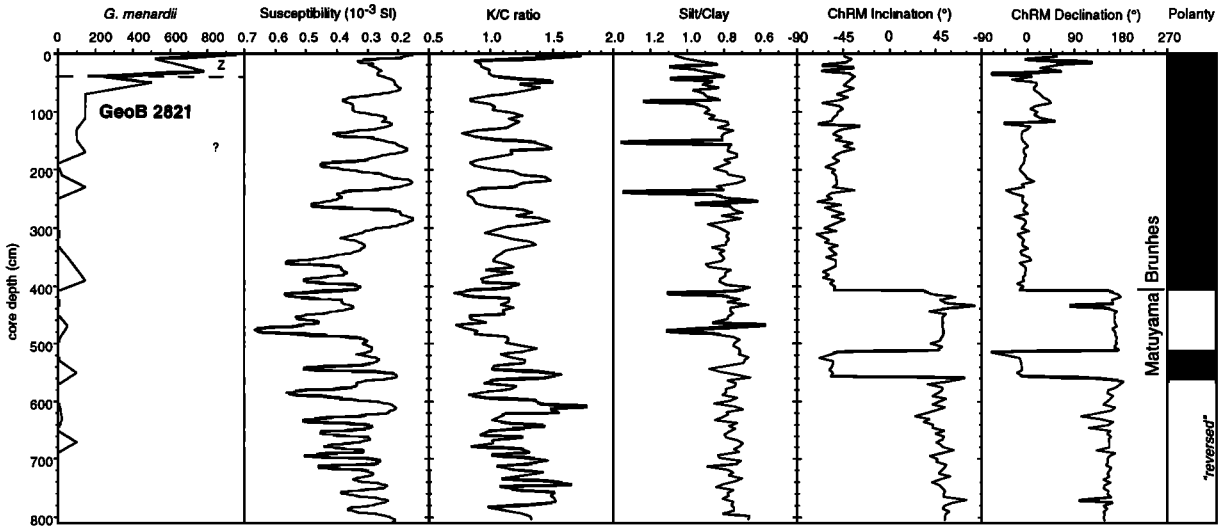
G. menardii
Susceptibility (10-3 SI)
K/C ratio
Silt/Clay
ChRM Inclination (°)
ChRM Declination (°)
Polarity
GeoB 2821
core depth (cm)
Z
?
Matuyama
Brunhes
"reversed"

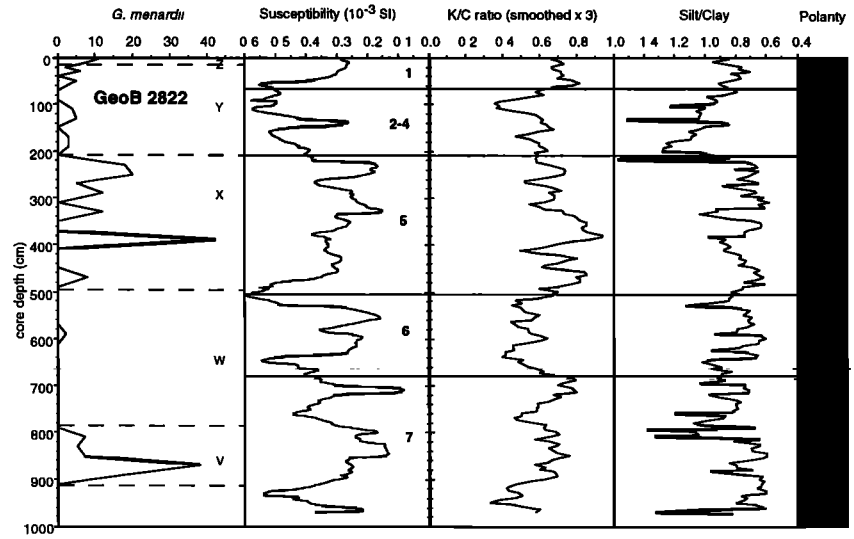
G. menardii
Susceptibility (10-3 SI)
K/C ratio (smoothed x 3)
Silt/Clay
Polarity
GeoB 2822
core depth (cm)
Z
Y
X
W
V
1
2-4
5
6
7

obliquity by 7.9 (7.4 - 8.2) kyr, a net lag of 4.5 kyr was applied for the tuning of magnetic susceptibility.

From the observation that faintly visible precessional peaks in the spectra gradually sharpened at both refinements of the age model the obliquity-tuned primary susceptibility record was filtered (15 - 47 kyr) to extract obliquity and precession cycles and matched to a composed target curve of normalized obliquity and precession.

2.3. Stratigraphy of GeoB 2822

According to *G. menardii* stratigraphy [*Jahn,* 1994] core GeoB 2822 reaches zone V of *Ericson and Wollin* [1968]. No isotope data were available to confirm these ages. Paleomagnetic measurements showed a uniform normal polarity throughout the core. The more detailed glacial-interglacial cycles revealed by the susceptibility record justify minor shifts of assumed stage boundaries Z/Y (isotope stages 1/2) and W/V (6/7). As in the other cores, kaolinite/chlorite and silt/clay (grain size) ratios generally correlate with the glacial-interglacial susceptibility record with the exception of stage 6 (Figure 2). Still, individual maxima in the susceptibility record within stage 6 correspond to maxima in the precessional index around 133, 160, and 185 ka. Minima can be related to precessional minima and peaks in the kaolinite/chlorite record. Nevertheless, absolute values for the minima in susceptibility are rather low for a glacial stage. Since this is a feature unparalleled in the other cores it cannot be satisfactorily explained by a common mechanism. Further detailed paleomagnetic investigations would be required to investigate this local, time-restricted phenomena. The final age models of all cores were obtained by linear interpolation between stratigraphic tie points (Figure 3).

3. Results and Discussion

3.1. Surface Distribution

Since kaolinite and chlorite are the proxy clay minerals commonly associated with propagation of NADW and AABW we use the kaolinite/chlorite ratio to delineate the extension of the deepwater masses as demonstrated in the approach of *Petschick et al.* [1996]. Additional sources of kaolinite should reflect in exceptionally high kaolinite/chlorite ratios. Kaolinite/chlorite ratios of the surface samples are depicted in Figure 1 and reveal some characteristic features of sediment input and distribution. Extremely high values between 10 and 80 are recorded off the mouth of the Rio Doce and confirm the role of this river as an important kaolinite source as already stated by *DeMelo et al.* [1975]. The highest values are found on the shelf and upper slope. However, it is important to note that enough river suspension is carried through the water column to keep kaolinite/chlorite ratios above 10 at 4000 m water depth. Even south of 25°, values exceed 2 below 4000 m water depth. Below 4000-4100 m in the Vema and Hunter Channels and the abyssal plains of the Argentine and Brazil Basins, kaolinite/chlorite ratios fluctuate from 0.5 to 1 and confirm the concept of AABW as a source and carrier of chlorite [*Biscaye* 1965; *Jones*, 1984; *Petschick et al.*, 1996]. Some of the river suspension introduced by the Rio Doce is carried south by the Brazil current. Scavenging and incorporation into fecal pellets are believed to remove most of the fine-grained material from the water column rather rapidly [*Deuser et al.*, 1983]. Accumulations of kaolinite-rich sediments are found on the continental slopes off Cabo Frio and with decreasing values above and on the Sao Paulo and Santos Plateaus from 2500 to 3000 m. Since the rivers south of Cabo Frio contain relatively little kaolinite the Rio Doce has to be regarded as the major source for these deposits [*Jones*, 1984].

A characteristic enrichment of kaolinite was also found at intermediate depths (3000-4000 m) on the RGR by *Chamley* [1975] and *Jones* [1984], with the maximum centered at 3300 to 3600 m. Such an enrichment is confirmed by our samples, which cover a depth range from 4500 to 2900 m water depth on the western flank of the RGR. A similar feature is observed on the transect from the eastern slope of the RGR to the Hunter Channel. East of the Hunter Channel toward the MAR kaolinite/chlorite ratios are lower (<1) at comparable water depths (Figure 1). Only on the top of the ridge maximum values of 1.0 are reached. This has important implications concerning the origin and propagation of kaolinite.

Jones [1984] proposed two models to explain the kaolinite enrichment at mid-depths of the RGR: (1) advective transport of kaolinite from low latitudes with NADW and (2) advection of kaolinite along isopycnals from resuspension of kaolinite-rich deposits on the Sao Paulo Plateau. Though he did not rule out the NADW transport model completely, the isopycnal mixing model was better suited to explain his observed clay mineral distribution. Kaolinite/chlorite ratios determined on our sediment surface sample set yield arguments for both transport models. The symmetrical nature of the kaolinite enrichment at middepths of both sides of the RGR could support the concept of advective transport of kaolinite from low latitudes with NADW. Consequently, similar kaolinite/chlorite ratios should be expected at comparable depths of the MAR. However, only a slight rise in kaolinite/chlorite values is recorded on the top, which may result from minor advection of kaolinite from low latitudes. On the other hand, although the transport of kaolinite to the western slope of the RGR along isopycnals from the Sao Paulo or Santos Plateaus may explain the kaolinite enrichment on the western side of the RGR, it is hard to imagine a mechanism that transports kaolinite-rich suspensions around or across the RGR to the "backside." To explain the symmetrical nature of the kaolinite enrichment on the RGR, we alternatively suggest the injection of kaolinite-rich suspensions into intermediate depths of the NADW off the mouth of the Rio Doce and short-distance transport southward instead of long-distance advection from lower latitudes. This idea is supported by high kaolinite/chlorite ratios down to 4000 m water depth off the river mouth, demonstrating that kaolinite-rich suspensions are able to reach deepwater levels. Injected at 20°S, these suspensions could be advected south with the NADW and be deposited on the first obstacle, which is the RGR.

Our results suggest that a substantial part of the terrigenous sedimentation on the RGR originates from freshwater input and

Figure 3. (opposite) Relative clay mineral percentages and kaolinite/chlorite ratios of cores GeoB 2110, GeoB 2821, and GeoB 2822 versus age. In order to produce a maximum glacial-interglacial contrast the cutoff for the shading of kaolinite/chlorite ratios was set at an average value of 1.0 for the cores within the North Atlantic Deep Water (NADW) (GeoB 2110 and GeoB 2821) and at 0.6 for the core within the Antarctic Bottom Water (AABW) (GeoB 2822). Isotope stages 1-7 [*Imbrie et al.*, 1984] are shaded.

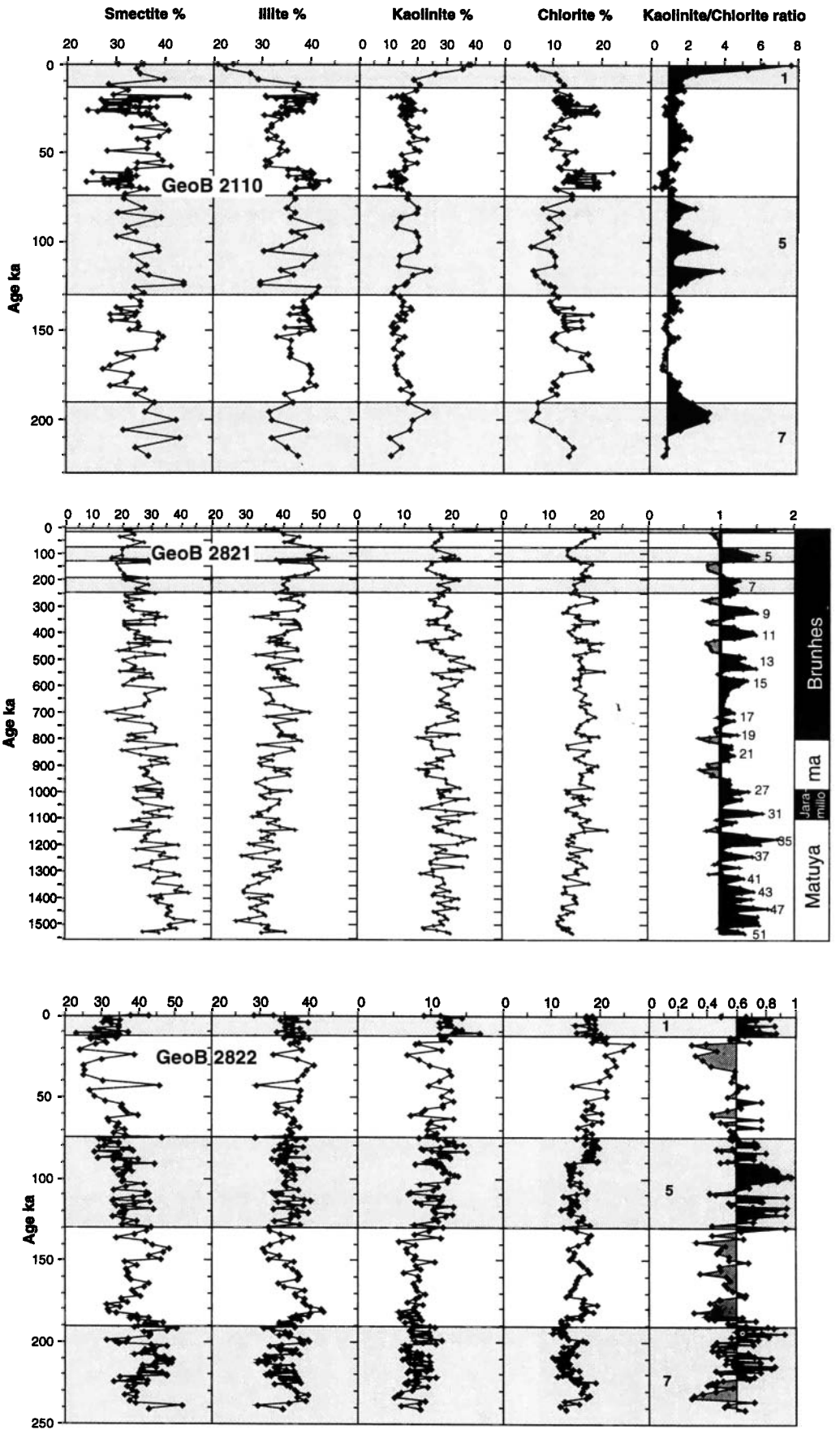
Smectite %
Illite %
Kaolinite %
Chlorite %
Kaolinite/Chlorite ratio
GeoB 2110
GeoB 2821
GeoB 2822
Age ka
Brunhes
ma
Jaramillo
Matuyama

suspension supply by the Rio Doce as evidenced by the kaolinite enrichment at intermediate depths of the RGR. The question arises of whether temporal variations in kaolinite supply primarily record pulses of fluvial discharge or rather represent varying intensities of short-distance NADW flow. To address this problem and look at the temporal variations of the kaolinite/chlorite ratios, we investigated three sediment cores.

3.2. Temporal Variations of Clay Mineral Input

Core GeoB 2110 was taken from 3000 m water depth at the continental slope above the Santos Plateau. Kaolinite/chlorite ratios in surface sediments reach a maximum at this depth (Figure 1) because of advection and deposition of kaolinite from the north with the Brazil current. Significant fluctuations of chlorite flux can be ruled out for this site because the only potential carrier of chlorite, AABW, always stayed well below these depths in the southwestern Atlantic [*Curry*, 1996]. Site GeoB 2110 shows highest kaolinite/chlorite ratios (4-8) in interglacial stages 1, 5 and 7 and lowest ratios (±1) in glacial sections (Figure 3). This is still in accordance with the model of *Jones* [1984], who proposed a southward transport of kaolinite from the mouth of the Rio Doce only during times of high sea level (interglacials) and a direct injection of the river load into intermediate and deepwater levels during times of low sea level (glacials). However, our surface data show high kaolinite/chlorite ratios down to 4000 m water depth also in recent (interglacial) sediments off the Rio Doce. Furthermore, if sea level exerts a major control on the input of kaolinite from the Rio Doce, minima in kaolinite/chlorite ratios could be also expected at the deep sites GeoB 2822 and 2821 during high stands. However, both deep sites show high kaolinite/chlorite ratios during interglacials. Therefore we hypothesize that a potential effect of sea level changes on the input of kaolinite to all our core sites is overridden by fluctuations in the total amount of river discharge.

Spectral analysis of the kaolinite/chlorite ratio of core GeoB 2110 (Figure 4) strengthens this assumption. Although the combined chronostratigraphy described above does not preserve the exact phase relation of different proxies, a Fourier transform yields information on spectral characteristics within the uncertainties of the dating procedure. The resulting spectrum indicates that there is a strong response of the kaolinite/chlorite ratio to precessional forcing. There is abundant evidence (summarized by *DeMenocal* [1995] and *Gingele et al.* [1998]) that low-latitude aridity-humidity cycles documented in eolian flux, monsoon intensity, or river discharge respond to variations in low-latitude insolation, which in turn result from Earth's orbital precession. Therefore we conclude that the kaolinite/chlorite ratio at site GeoB 2110 is significantly influenced by low-latitude river discharge.

The spectrum also documents 100 and 41 kyr variance (Figure 4). The dual nature of high- and low-latitude forcing of low-latitude climate has been recognized by *DeMenocal* [1995] in various sites around the African continent. Mechanisms transporting high-latitude signals, namely the pronounced 100 and 41 kyr cycles, to low latitudes are believed to be cooling North Atlantic surface water and fostering shifts in atmospheric circulation and migration of vegetation belts. Especially the 100 kyr frequency of eccentricity is prominent in many aridity-humidity records [*Pastouret et al.*, 1978; *DeMenocal et al.*, 1993; *Gingele et al.*, 1998].

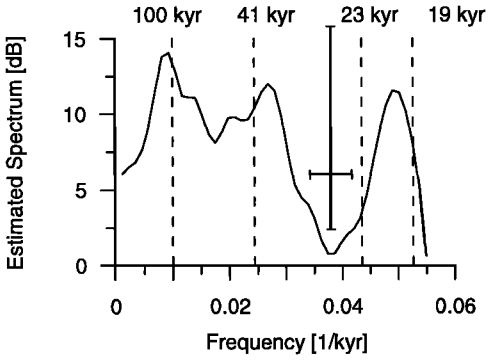

Figure 4. Spectral analysis of kaolinite/chlorite ratio of core GeoB 2110. In addition to spectral peaks near 100 and 41 kyr, strong response to precessional forcing becomes visible in the modified periodogram calculated by Lomb-Scargle Fourier transform using a Welch window. The cross depicts 6 dB bandwidth (horizontal) and 80% confidence interval (vertical).

Core GeoB 2822 from the eastern terrace of the Vema Channel (4300 m water depth) is believed to represent sedimentation within the AABW during interglacial as well as glacial times. The advection of chlorite from the south is documented in the lowest kaolinite/chlorite ratios (<1) of all investigated cores. Although of low amplitude, a significant glacial-interglacial pattern in the kaolinite/chlorite signal can be recognized, with higher values in the interglacial sections (Figure 3). Evidence from grain size and sediment texture from the area [*Johnson and Rasmussen*, 1984; *Massé et al.*, 1994] indicates a more vigorous flow of AABW at the transition from warm to cold periods and within glacials. Increased advection of chlorite with intensified AABW activity during glacials could explain the observed fluctuations in kaolinite/chlorite ratios of core GeoB 2822. Since the site is well below the direct influence of NADW the advection of kaolinite from low latitudes is an unlikely source for GeoB 2822. Therefore we remain with the Rio Doce as the primary kaolinite source also for this core.

Cyclic variations are also recorded in kaolinite/chlorite ratios of core GeoB 2821 (Figure 3). High values correspond to lows in the susceptibility record (Figure 2) and thus interglacial stages (Figure 3). The clay mineral proxy fluctuates in tune with many paleoclimate proxies dominated by high-latitude orbital forcing. A shift in the dominant period of variation from 41 to 100 kyr is visible near 1000 ka (Figure 3).

Cross-spectral analysis of the kaolinite/chlorite ratio of core GeoB 2821 was performed versus the reversed SPECMAP $\delta^{18}O$ stack and reversed $\partial^{18}O$ record of ODP 677 for the past 500 kyr and and versus the reversed $\partial^{18}O$ record of ODP 677 for the past 1500 kyr. It appears that the clay mineral proxy is coherent with global ice volume in the 41 and 100 kyr periods of obliquity and eccentricity (Table 2 and Figures 5 and 6). Resolution and sedimentation rates of the core are too low to investigate a precession-related variability. Moreover, statistical data (Table 2) for the complete kaolinite/chlorite record are difficult to interpret since significant variation in the 100 kyr band occurs only during the past 350 kyr, where 41 kyr cycles, dominating the older

Table 2. Data of Cross Spectral Analysis

	100 kyr^{-1} Band		41 kyr^{-1} Band		23 kyr^{-1} Band		T,	Δt,
	k	°Phi	k	°Phi	k	°Phi	kyr	kyr
			Versus Reversed SPECMAP Stack $\delta^{18}O$					
Kaolinite/chlorite (GeoB 2821-1),.0-500 ka	0.99	-5±3(5)	0.99	-32±3(5)	-	-	500	5.0
Maximum ∂D Vostok ice core [*Jouzel et al.*, 1994]		-	0.93	-46±12	-	-	220	1.0
%NADW index [*Raymo et al.*, 1990]	0.87	16±15	0.86	5±16	0.83	41±17	400	3.0
Kaolinite/chlorite 43° S [*Diekmann et al.*, 1996]	0.96	-6±7	0.87	11±14	-	-	388	2.0
			Versus Reversed ODP677 $\delta^{18}O$					
Kaolinite/chlorite (GeoB 2821-1), 0-1500 ka	0.96	-33±8(13)	0.94	-31±10(15)	-	-	1525	5.0
Kaolinite/chlorite (GeoB 2821-1), 0-500 ka		-2±2(3)	0.95	-42±10(13)	-	-	500	5.0

Abbreviations are k, coherency; °Phi, phase angle with 80% confidence interval (in parentheses 95%); T, maximum age used in the calculation; Δt, sample interval. The $\partial^{18}O$ SPECMAP stack was taken from *Imbrie et al.* [1984], and the $\partial^{18}O$ record Ocean Drilling Program Site (ODP) 677 from *Shackleton et al.* [1990].

section, are reduced (Figure 5). As a consequence of this reflection of the mid-Pleistocene climate transition [e.g., *Ruddiman et al.*, 1989] we concentrate on the section from 0 to 500 ka for the 100 kyr cycle and make use of the whole record for the 41 kyr period. As statistical data (Table 2) and phase wheels (Figure 6) indicate, maxima in GeoB 2821 kaolinite/chlorite ratios lead maxima in NADW flux by 5800 years in the 100 kyr cycle (0 to 500 ka) and 4100 years in the 41 kyr cycle (0 to 500 and 0 to 1500 ka). These results are consistent with characteristic values of early proxy responses in the Southern Hemisphere [*Imbrie et al.*, 1993].

NADW production and propagation have varied in orbital time scales, though the relation to climate is not simple [*Curry*, 1996]. In the western Atlantic (Ceara Rise), only NADW was recorded in some peak interglacials, whereas in some glacials, southern source deepwater reached 3200 m water depth [*Curry*, 1996]. Investigations in the eastern part of the South Atlantic [*Diekmann et al.*, 1996] have shown that the propagation and southward extension of northern source deepwater (NADW) were more pronounced during interglacials, thus providing more kaolinite during warm periods. At first glance, kaolinite/chlorite ratios of core GeoB 2821 fit nicely in the concept of alternating intensities of interglacial NADW [*Diekmann et al.*, 1996] and glacial AABW [*Massé et al.*, 1994] flow. Within the error margins (Table 2), phase angles of kaolinite/chlorite ratios in the 100 kyr band of eccentricity are similar in the eastern and western Atlantic. The implications for the RGR are that either the kaolinite/chlorite ratio is controlled by changes in deepwater flux or that the high-latitude forcing mechanisms, which control deepwater flux and low-latitude climate in the eccentricity band, do not show a significant time lag. However, there are strong arguments opposing an exclusively deepwater-controlled clay mineral supply for sites GeoB 2821 as well as GeoB 2822.

First, AABW activity was strongly reduced after 350 [*Massé et al.*, 1994] or 275 ka [*Johnson and Rasmussen*, 1984], respectively, which would lead to rising kaolinite/chlorite ratios from 350 ka to present. Instead, we find decreasing kaolinite/chlorite ratios in core GeoB 2821.

Second, in the 41 kyr band, maxima of kaolinite/chlorite ratios of core GeoB 2821 significantly lead minima in ice volume, maxima in %NADW flux [*Raymo et al.*, 1990] and maxima in kaolinite/chlorite ratios in the eastern South Atlantic [*Diekmann et al.*, 1996] (statistical data in Table 2). Moreover, the phase angle of kaolinite/chlorite ratios of core GeoB 2821 in the 41 kyr period is close to the maxima of ∂D (deuterium) in the Vostok ice core [*Jouzel et al.*, 1994]. Maxima in the ∂D record indicate periods of increased atmospheric temperatures in Antarctica [*Waelbroeck et al.*, 1995], which are related to intensified evaporation and precipitation in lower latitudes. Consequently, we suggest that temporal changes in the kaolinite/chlorite ratio of the RGR cores may be rather interpreted as an atmospheric signal of precipitation and river input than as a proxy of deepwater fluctuations.

4. Paleoceanographic and Paleoclimatic Implications

Summarizing the evidence from clay mineralogy, grain size, and magnetic susceptibility, we find that the flux of terrigenous matter on the RGR shows cyclic variations at least in the 100 and 41 kyr periods. Interglacial stages are characterized by the deposition of fine-grained, kaolinite-rich terrigenous matter of low magnetic susceptibility. They record periods of increased humidity on the South American mainland and runoff of the Rio Doce. High fluvial discharge was also recorded for the Orinoco and Amazon Rivers during interglacials [*Bowles and Fleischer*, 1985]. *Clapperton* [1993] reported more humid conditions for interglacial stage 5 in Patagonia. The concept of increased humidity in interglacial periods (100 kyr period) is in accordance with results from multiple investigations on the African continent (summary in *DeMenocal* [1995]). Runoff of major African rivers and monsoon intensity fluctuates in the 100 kyr period of global ice volume and 23 kyr period of low-latitude insolation [*Pastouret et al.*, 1978; *Zachariasse et al.*, 1984; *Rossignol Strick*, 1985; *Pokras*, 1987; *Gingele et al.*, 1998]. Our data from the RGR yield similar results for the South American continent at

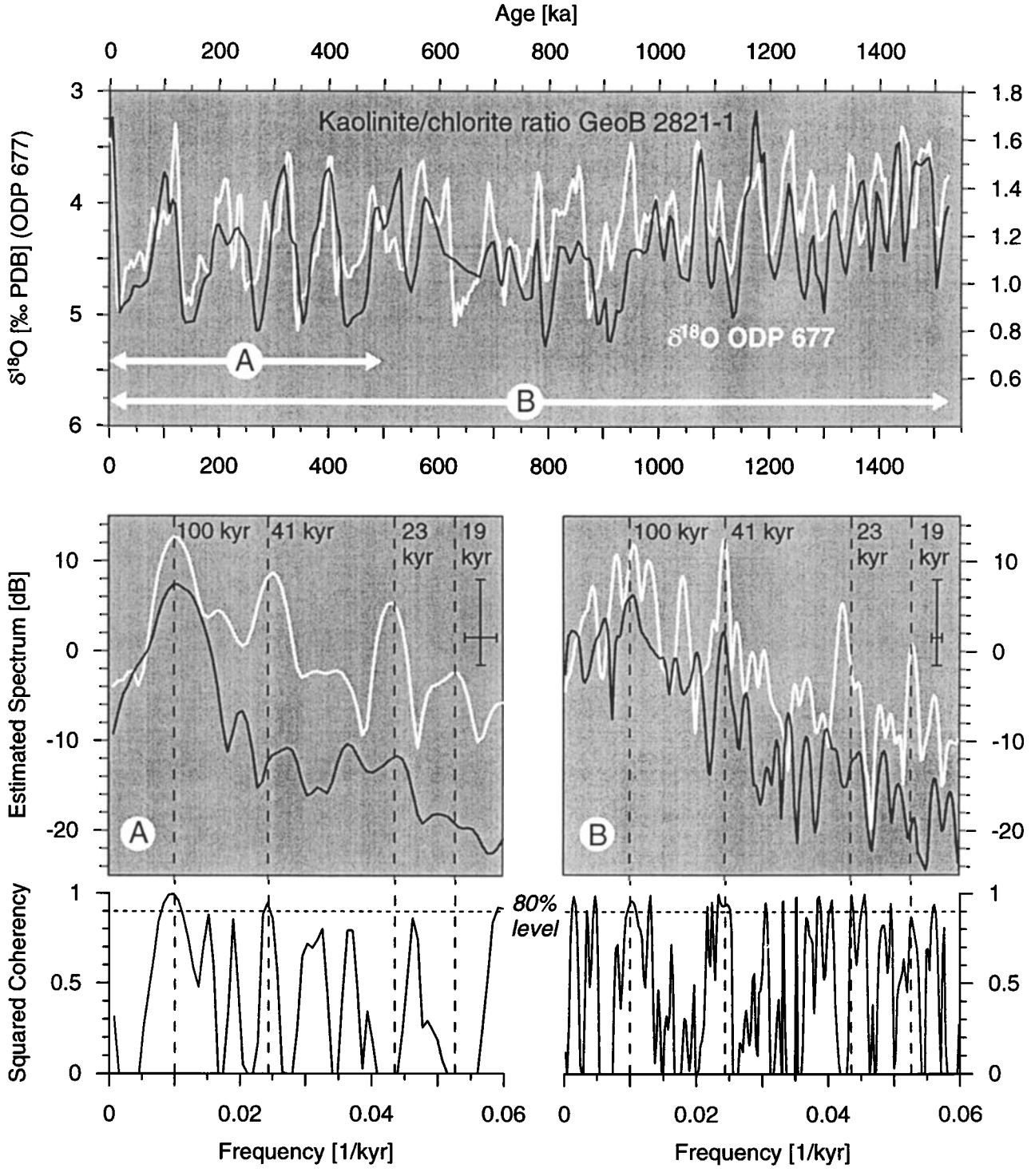

Figure 5. Cross-spectral analysis of kaolinite/chlorite ratio of core GeoB 2821 (black lines) and the reversed $\partial^{18}O$ record of Ocean Drilling Program (ODP) Site 677 (white lines) [*Shackleton et al.*, 1990]. While the past 500 kyr are dominated by eccentricity-related 100 kyr cycles (A), an increased amount of variance in the obliquity band near 41 kyr appears in the spectra of the 0-1500 ka records (B). Both time series are interpolated to 5 kyr steps, the average time resolution of the kaolinite/chlorite record of GeoB 2821. The analysis was performed using *Welch's* [1967] overlapped segment average (WOSA) procedure with two overlapping segments and a Welch window. The sign of the $\partial^{18}O$ record of ODP 677 was inverted to attain directly interpretable phase relations. Crosses depict 6 dB bandwidth and 80% confidence interval. The resulting negative phase angles shown in Table 2 indicate a lead with respect to $\partial^{18}O$. High squared coherency is calculated in the 100 and 41 kyr band.

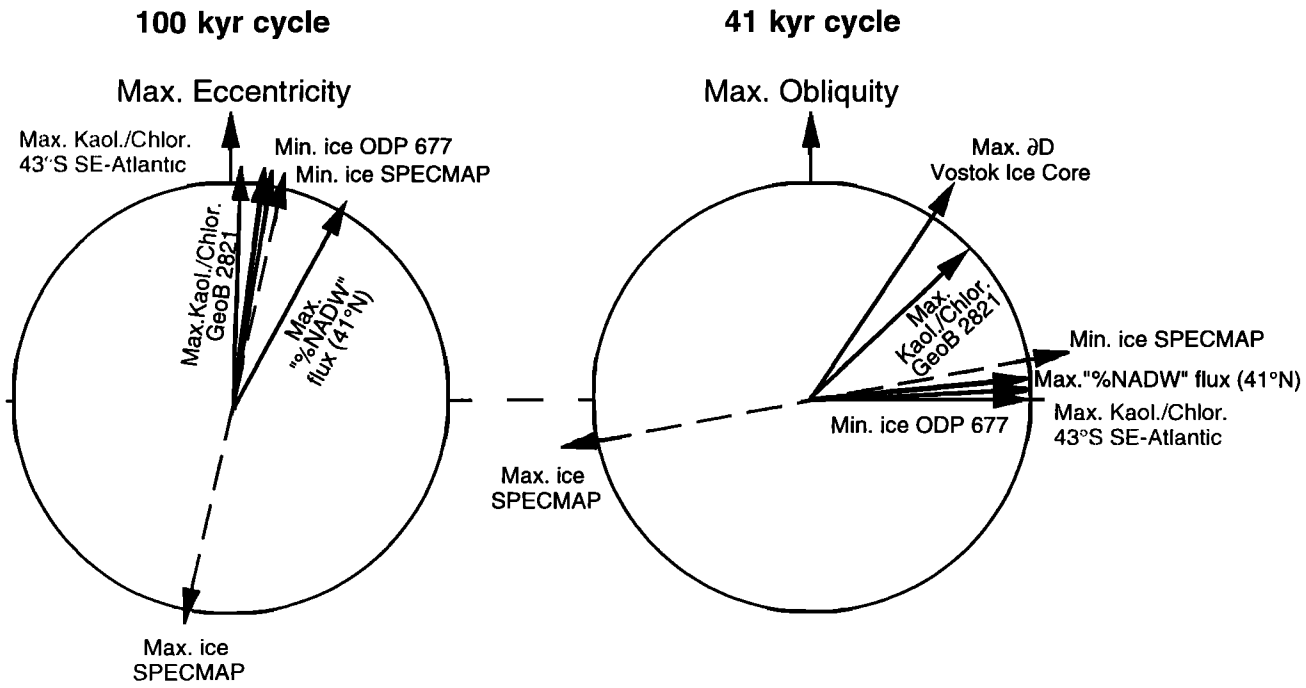

Figure 6. Phase relationships between kaolinite/chlorite ratios of core GeoB 2821 (0-500 ka), % NADW flux [*Raymo et al.*, 1990], kaolinite/chlorite ratios of a core 43°S in the SE Atlantic [*Diekmann et al.*, 1996], and the maximum of∂D (deuterium) in the Vostok ice core [*Jouzel et al.*, 1994] in the 100 and 41 kyr periods of eccentricity and obliquity (statistical data see Table 2).

20°S in the 100 and 41 kyr periods. In core GeoB 2110 the resolution is sufficient to record fluctuations of kaolinite flux in the 23 kyr precessional band. They are believed to represent humidity and discharge variations of the Rio Doce initiated by low-latitude insolation changes.

Minima in the precessional index correspond to increased input of kaolinite and may be interpreted in terms of higher humidity in the drainage area of the Rio Doce. It is interesting to note that at about the same latitude west of the Andes in northern Chile, precession-related humidity/aridity cycles are recorded, which show exactly the opposite pattern [*Lamy, et al.* 1998]. There, maxima in the precessional index correspond to more humid conditions in the sediment record. Increased precipitation there is related to a shift in the position of the southern westerlies and indicates a nonsynchronous behavior of South American paleoclimate on an orbital timescale.

Glacial stages are characterized by maxima in magnetic susceptibility, illite, and grain size (more silt) and lows in kaolinite supply. Cold and dry conditions have been reported for the headwaters of the Rio Doce during the last glacial [*Behling and Lichte*, 1997]. The lack of dilution by fine-grained river suspensions, a more vigorous AABW flow, and the increased input of silt-sized dust, rich in magnetic particles and illite, may have combined to form the terrigenous signal of the cold periods. Previous studies have shown that major fluctuations in dust flux appear to be of global significance with maximum inputs during cold and arid periods [*Clemens and Prell*, 1990; *DeMenocal et al.*, 1993]. A potential source area for dust in the southwestern Atlantic is Patagonia. Patagonian dust is derived from loess deposits, which contain a high percentage of titanomagnetite and illite [*Teruggi*, 1957; *Bonorino*, 1966; *Zarate and Balsi*, 1993]. Although insignificant for the total terrigenous mass balance, the input of Patagonian dust in cold periods could selectively enhance the susceptibility signal preformed by glacial carbonate dissolution events. It may also contribute to an illite enrichment of glacial core sections.

It appears that the composition of the terrigenous matter on the Brazilian slope and also on the RGR responds to changes in humidity/aridity on the adjacent South American continent rather than to variations in deepwater advection. The dual influence of high- and low-latitude forcing on the paleoclimate in the Brazilian hinterland is believed to result in periodical discharge of the Rio Doce. Consequently, the supply and deposition of kaolinite on the slope and the RGR are recorded for the major Milankovitch periodicities.

Multiple potential sources complicate the interpretation of the main clay mineral components smectite and illite. Nevertheless, individual peaks in the downcore record of smectite in core GeoB 2821 are frequently associated with maxima in kaolinite/chlorite ratios and thus with warm and humid periods, whereas illite shows a reciprocal pattern. More evident is a long-term trend in smectite and illite percentages (Figure 3). Illite percentages increase while smectite percentages, as well as average kaolinite/chlorite ratios, decrease from 1500 ka to present. If the paleoclimatic interpretation of the clay mineral proxies is correct, a trend toward more arid and glacial conditions during the Pleistocene is evident. These findings are consistent with results from the African continent [*DeMenocal*, 1995]. Here proxies for African aridity reconstructed from various ODP sites around the continent show a gradual trend toward more arid and cooler conditions from the Pliocene to present with prominent shifts around 2800, 1700, and 1000 ka [*DeMenocal*, 1995].

5. Conclusions

Clay mineral analyses revealed that the Rio Doce (Brazil) is a major source of kaolinite for marine sediments at 20°-30°S in the western Atlantic. Characteristic enrichments of kaolinite are observed at intermediate depths of the continental slope and on the flanks of the RGR at 3000-4000 m water depth.

The supply of kaolinite with NADW is minor as evidenced by the comparison of kaolinite/chlorite ratios from the MAR and the RGR. Consequently, patterns of terrigenous sedimentation in this part of the Atlantic record climatic conditions on the South American hinterland.

Low-latitude insolation fosters periodical discharge of the Rio Doce in the precessional 23 kyr band, as evidenced in kaolinite/chlorite ratios on the Brazilian slope. Cyclic variations of kaolinite/chlorite ratios on the slope and in a core from the western flank of the RGR are coherent with global ice volume in the 41 and 100 kyr periods. They are also believed to record fluctuations in the discharge of the Rio Doce and mirror humidity conditions on the adjacent South American hinterland. Humid periods are coeval with warm interglacial phases, whereas arid periods correspond to cold, glacial stages. The dual mode of high- and low-latitude forcing of low latitude climate is consistent with similar findings from the African continent. A longtime decrease in smectite content and kaolinite/chlorite ratios from 1500 ka to present is believed to document a trend toward more arid and cooler climate conditions for subtropical southern latitudes of South America.

Acknowledgments. The dedication and effort of crew and master of R/V *Meteor* is greatly acknowledged. We are grateful to F. Bassinot and D. Dobson for constructive reviews and helpful comments. All the data used in this manuscript are archived in the information system PANGAEA/SEPAN (www.pangaea.de). F. Schmieder was supported by the Deutsche Forschungsgemeinschaft in the framework of Graduiertenkolleg 221. This is contribution 249 of special research project SFB 261.

References

Balsam, W. L., B. L. Otto-Bliesner, and B. C. Deaton, Modern and Last Glacial Maximum eolian sedimentation patterns in the Atlantic Ocean interpreted from sediment iron oxide content, *Paleoceanography, 10,* 493-507, 1995.

Behling, H., and M. Lichte, Evidence of dry and cold climactic conditions at glacial times in tropical southeastern Brazil, *Quat. Res., 48,* 348-358, 1997.

Berger, A., and M.F. Loutre, Insolation values for the climate of the last 10 million years, *Quat. Sci. Rev., 10,* 297-317, 1991.

Bickert, T., Rekonstruktion der spätquartären Bodenwasserzirkulation im östlichen Südatlantik über stabile Isotope benthischer Foraminiferen, *Ber. Fachbereich Geowiss. Univ. Bremen, 27,* 205, 1992.

Biscaye, P. E., Mineralogy and sedimentation of recent deep-sea clay in the Atlantic Ocean and adjacent seas and oceans, *GSA Bull., 76,* 803-832, 1965.

Bleil, U., and Cruise Participants, Report and preliminary results of *Meteor* cruise 23/2 Rio de Janeiro - Recife, 27.2.1993 - 19.3.1993, *Ber. Fachbereich Geowiss. Univ. Bremen, 43,* 133, 1993.

Bleil, U., and Cruise Participants, Report and preliminary results of *Meteor* cruise 29/2 Montevideo - Rio de Janeiro, 15.7.1994 - 08.08.1994, *Ber. Fachbereich Geowiss. Univ. Bremen, 59,* 153, 1994.

Bonorino, F. G., Soil clay mineralogy of the Pampa Plains, Argentia, *J. Sediment. Res., 36,* 1026-1035, 1966.

Bowles, F. A., and P. Fleischer, Orinoco and Amazon River sediment input to the eastern Caribbean Basin, *Mar. Geol., 68,* 53-72, 1985.

Boyle, E. A., Cadmium: Chemical tracer of deep-water paleoceanography, *Paleoceanography, 3,* 471-489, 1988.

Boyle, E. A., A comparison of carbon isotopes and cadmium in the modern and glacial maximum ocean: Can we account for the discrepancies? *Carbon Cycling in the Glacial Ocean: Constraints on the Ocean's Role in Global Change, NATO ASI Ser. C,* vol. 117, edited by R. Zahn et al., pp. 105-144, Springer, New York, 1994.

Chamley, H., Influence des courants profonds au large du bresil sur la sedimentation argeleuse recent, *IXe Congr. Int. Sedimentol. Nice, Abstracts,* 13-19, 1975.

Clapperton, C. M., *Quaternary Geology and Geomorphology of South America,* 779 pp., Elsevier, New York, 1993.

Clemens, S. C., and W. L. Prell, Late Pleistocene variability of Arabian Sea summer monsoon winds and continental aridity: Eolian records from the lithogenic component of deep-sea sediments, *Paleoceanography, 5,* 109-145, 1990.

Curry,W. B., Late Quaternary deep circulation in the western equatorial Atlantic, *The South Atlantic: Present and Past Circulation,* edited by G. Wefer et al., pp. 577-598, Springer-Verlag, New York, 1996.

Curry, W. B., J. C. Duplessy, L. D. Labeyrie, and N. J. Shackleton, Changes in the distribution of $\partial^{13}C$ of deep water $\sum CO_2$ between the last glaciation and the Holocene, *Paleoceanography, 3,* 317-341, 1988.

Damuth, J. E., Late Quaternary sedimentation in the western equatorial Atlantic, *Geol. Soc. Am. Bull., 88,* 695-710, 1977.

DeMelo, U., C. P. Summerhayes, and J. P. Ellis, Salvador to Vitoria, southeastern Brazil, IV, *Contrib. Sedimentol., 4,* 78-116, 1975.

DeMenocal, P., Plio-Pleistocene African climate, *Science, 270,* 53-59, 1995 .

DeMenocal, P. B., W. F. Ruddiman, and E. M. Pokras, Influences of high- and low-latitude processes on African terrestrial climate: Pleistocene eolian records from equatorial Atlantic Ocean drilling program site 663, *Paleoceanography, 88,* 209-242, 1993.

Deuser, W. G., P. G. Brewer, T. D. Jickells, and R. F. Commeau, Biological control of the removal of abiogenic particles from the surface ocean, *Science, 219,* 388-391, 1983.

Diekmann, B., R. Petschick, F. X. Gingele, D. K. Fütterer, A. Abelmann, R. Gersonde, U. Brathauer, and A. Mackensen, Clay mineral fluctuations in late Quaternary sediments of the southeastern South Atlantic: Implications for past changes of deepwater advection, *The South Atlantic: Present and Past Circulation,* edited by G. Wefer et al., pp. 621-644, Springer-Verlag New York, 1996.

Duplessy, J. C., N. J. Shackleton, R. G. Fairbanks, L. D., Labeyrie, D. Oppo, and N. Kallel, Deep water source variations during the last climatic cycle and their impact on the global deep water circulation, *Paleoceanography, 3,* 343-360, 1988.

Ericson, D. B., and G. Wollin, Pleistocene climates and chronology in deep-sea sediments, *Science, 162,* 1227-1234, 1968.

Gingele, F. X., P. J. Müller, and R. R. Schneider, Orbital forcing of freshwater input in the Congo-Fan area: Clay mineral evidence from the last 200 kyr, *Paleogeogr. Paleoclimatol. Paleoecol., 138,* 17-26, 1998.

Griffin, J. J., H. Windom, and E. D. Goldberg, The distribution of clay minerals in the World Ocean, *Deep Sea Res. Oceanogr. Abstr., 15,* 433-459, 1968.

Heath, G. R., and N. G. Pisias, A method for the quantitative estimation of clay minerals in North Pacific deep-sea sediments, *Clays Clay Miner., 27,* 175-184, 1979.

Imbrie, J., J. D. Hays, D. G. Martinson, A. McIntyre, and A. C. Mix, The orbital theory of Pleistocene climate: Support from a revised chronology of the marine $\partial^{18}O$ record, in *Milankovitch and Climate, Part 1,* edited by A. Berger et al., pp. 269-305, D. Reidel, Norwell, Mass., 1984.

Imbrie J., et al., On the structure and origin of major glaciation cycles, 2, The 100,000-year cycle, *Paleoceanography, 8,* 699-735, 1993.

Jahn, B., Menardii stratigraphy, in *Report and Preliminary Results of Meteor Cruise 29/2 Montevideo - Rio de Janeiro, 15.7.1994 - 08.08.1994.*, edited by U. Bleil and Cruise Participants, *Ber. Fachbereich Geowiss. Univ. Bremen, 59,* 153, 1994.

Johnson, D. A., and K. A. Rasmussen, Late Cenozoic turbidite and contourite deposition in the southern Brazil Basin, *Mar. Geol., 58,* 225-262, 1984.

Jones, G. A., Advective transport of clay minerals in the region of the Rio Grande Rise, *Mar. Geol., 58,* 187-212, 1984.

Jones, G. A., and D. A. Johnson, Displaced Antarctic diatoms in Vema Channel sediments: Late Pleistocene/Holocene fluctuations in AABW flow, *Mar. Geol., 58,* 59-88, 1984.

Jouzel, J., C. Lorius, J. R. Petit, C. Ritz, M. Stievenard, P. Yiou, N. I. Barkov, V. M. Kotlyakov, and V. Lipenkov, The climatic record from Antarctic ice now extends back to 220 kyr BP, in *Long-term Climatic Variations, NATO ASI Ser., I,* vol. 22, edited by J.-C. Duplessy and M.-T. Spyridakis, pp. 213-237, Springer, New York, 1994.

Lamy, F., D. Hebbeln, and G. Wefer, Late Quaternary precessional cycles of terrigenous sediment input off the northern

Chico, Chile (27.5°S) and paleoclimatic implications, *Paleogeogr. Paleoclimatol. Paleoecol., 141*, 233-251, 1998.

Lomb, N.R., Least-squares frequency analysis of unequally spaced data, *Astrophys. Space Sci., 39*, 447-462, 1976.

Mackensen, A., D. K. Fütterer, H. Grobe, and G. Schmiedl, Benthic foraminiferal assemblages from the eastern South Atlantic Polar Front region between 35° and 57°S: Distribution, ecology and fossilization potential, *Mar. Micropaleontol., 22*, 33-69, 1993.

Mackensen, A., H. Grobe, H.-W. Hubberten, and G. Kuhn, Benthic foraminiferal assemblages and the ∂^{13}C-signal in the Atlantic sector of the Southern Ocean, *Carbon Cycling in the Glacial Ocean: Constraints on the Ocean's Role in Global Change, NATO ASI Ser. C*, vol. 117, edited by R. Zahn et al., pp. 105-144, Springer, New York, 1994.

Massé, L., J.-C. Faugères, M. Bernat, A. Pujos, and M.-L. Mézerais, A 600,000-year record of Antarctic Bottom Water activity inferred from sediment textures and structures in a sediment core from the Southern Brazil Basin, *Paleoceanography, 9*, 1017-1026, 1994.

Mulitza, S., Stratigraphy, in *Report and Preliminary Results of Meteor Cruise 23/2 Rio de Janeiro - Recife, 27.2.1993 - 19.3.1993*, edited by U. Bleil, and Cruise Participants, *Ber. Fachbereich Geowiss. Univ.Bremen, 43*, 133, 1993.

Oppo, D. W., and Y. Rosenthal, Cd/Ca changes in a deep Cape Basin core over the past 730,000 years: Response of circumpolar deepwater variability to Northern Hemisphere ice sheet melting?, *Paleoceanography, 9*, 661-675, 1994.

Pastouret, L., H. Chamley, G. Delibrias, J. C. Duplessy, and J. Thiede, Late Quaternary climatic changes in western tropical Africa deduced from deep-sea sedimentation off Niger delta, *Oceanol. Acta, 1*, 217-232, 1978.

Pätzold, J., and Cruise Participants, Berichte und erste Ergebnisse über die *Meteor*-Fahrt M15/2 Rio de Janeiro - Vitoria, 18.1.1991 - 7.2.1991, *Ber. Fachbereich Geowiss. Univ. Bremen, 17*, 46, 1993.

Peterson, R. G., and L. Stramma, Upper-level circulation in the South Atlantic Ocean, *Progr. Oceanogr., 26*, 1-81, 1990.

Petschick, R., G. Kuhn, and F. X. Gingele, Clay mineral distribution in surface sediments of the South Atlantic: Sources, transport and relation to oceanography, *Mar. Geol., 130*, 203-229, 1996.

Pokras, E. M., Diatom record of late Quaternary climatic change in the eastern equatorial Atlantic and tropical Africa, *Paleoceanography, 2*, 273-286, 1987.

Raymo, M. E., W. F. Ruddiman, N. J. Shackleton, and D. W. Oppo, Evolution of Atlantic-Pacific d^{13}C gradients over the last 2.5 m.y., *Earth Planet. Sci. Lett., 97*, 353-368, 1990.

Robinson, S. G., Applications for whole-core magnetic susceptibility measurements of deep-sea sediments, *Proc. Ocean Drill. Program Sci. Results, 115*, 737-771, 1990.

Rossignol-Strick, M., Mediterranean Quaternary sapropels: An immediate response of the African monsoon to variation of insolation, *Paleogeogr. Paleoclimatol. Paleoecol., 49*, 237-263, 1985.

Ruddiman, W.F., M.E. Raymo, D.G. Martinson, B.M. Clement, and J. Backman, Pleistocene evolution: Northern Hemisphere ice sheets and North Atlantic ocean, *Paleoceanography, 4*, 353-412, 1989.

Scargle, J.D., Studies in astronomical time series analysis, II, Statistical aspects of spectral analysis of unevenly spaced data, *Astrophys. J., 263*, 835-853, 1982.

Scargle, J.D., Studies in astronomical time series analysis, III, Fourier transforms, autocorrelation functions, and cross-correlation functions of unevenly spaced data, *Astrophys. J., 343*, 847-887, 1989.

Schmiedl, G., and A. Mackensen, Late Quaternary paleoproductivity and deep water circulation in the eastern South Atlantic Ocean: Evidence from benthic foraminifera, *Paleogeogr. Paleoclimatol. Paleoecol., 130*, 43-80, 1997.

Schulz, M., and K. Stattegger, Spectrum: Spectral analysis of unevenly spaced paleoclimatic time series, *Comp. Geosci., 23*, 929-945, 1997.

Shackleton, N. J., A. Berger, and W. R. Peltier, An alternative astronomical calibration of the lower Pleistocene timescale based on ODP site 677, *Trans. R. Soc. Edinburgh Earth Sci., 81*, 251-261, 1990.

Teruggi, M. E., The nature and origin of Argentine Loess, *J. Sedimentol. Petrol., 27/3*, 322-332, 1957.

von Dobeneck, T., and F. Schmieder, Using rock magnetic proxy records for orbital tuning and extended time series analysis into the super and sub-Milankovitch bands, *Proxies in Paleoceanography*, edited by G. Fischer and G. Wefer, Springer, New York, in press, 1998.

Waelbroeck, C., J. Jouzel, L. Labeyrie, C. Lorius, M. Labracherie, M. Stievenard, and N. I. Barkov, A comparison of the Vostok ice deuterium record and series from Southern Ocean core MD 88-770 over the last two glacial-interglacial cycles, *Clim. Dyn., 12*, 113-123, 1995.

Wefer, G., and Cruise Participants, Report and preliminary results of *Meteor*-cruise M34/3 Walvis Bay - Recife, 21.02. - 17.03.1996, *Ber. Fachbereich Geowiss. Univ. Bremen, 79*, 168, 1996.

Zachariasse, W. J., R. R. Schmidt, and R. J. W. Van Leuwen, Distribution of foraminifera and calcareous nannoplankton in Quaternary sediments of the eastern Angola Basin in response to climatic and oceanic fluctuations, *Neth. J. Sea Res., 17*, 250-275, 1984.

Zarate, M., and A. Balsi, Late Pleistocene-Holocene eolian deposits of the southern Buenos Aires province, Argentina: A preliminary model, *Quat. Int., 17*, 15-20, 1993.

F. X. Gingele, Baltic Sea Research Institute, Seestrasse 15, D-18119 Warnemünde, Germany. (e-mail: franz.gingele@io-warnemuende.de)

R. Petschick, Fachbereich Geowissenschaften, Universität Frankfurt Senckenberganlage 32-34, D-60325 Frankfurt, Germany.

C. Rühlemann, F. Schmieder, and T. von Dobeneck, Fachbereich Geowissenschaften, Universität Bremen, Bibliotheksstrasse, D-28334 Bremen, Germany.

(Received April 9, 1998;
revised October 23, 1998;
accepted October 27, 1998.)